

# Photon Counting

James Amarel and Ben Miller

March 17, 2017

## 1 Goal

To measure a probability distribution for the number of photon counts detected by a photomultiplier tube, through the photoelectric effect, in the case of a constant intensity light source and a pseudothermal light source.

## 2 Introduction/Background

Stimulated emission within a laser produces a beam of photons of uniform phase and amplitude, but when this source is of low intensity and is incident on the cathode plate of a photomultiplier tube (PMT), the measured signal is an irregular train of output pulses. This is because a PMT functions via the photoelectric effect by converting incoming photons into photoelectrons, but the probability of an incoming photon ejecting an electron is entirely stochastic in nature. Only a fraction of incident photons lead to the creation of a photoelectron, referred to as the quantum efficiency (QE), which is a wavelength dependent property of the device.

For a time interval  $\delta t$  much less than the time between photoejections, ensuring that we need only consider recording a count of either 1 or 0, the probability of obtaining a single count is

$$P(1, \delta t) = \lambda \delta t \quad (1)$$

where  $\lambda$  is the rate of incoming photons. Then, the probability of obtaining  $n$  counts in a time interval  $T$ , where  $T \gg \delta t$  and we let  $N$  be defined by  $T = N\delta t$ , is given by

$$P(n, N\delta t) = \binom{N}{n} (\lambda \delta t)^n (1 - \lambda \delta t)^{N-n}. \quad (2)$$

Where  $(1 - \lambda \delta t)$  is the probability of not getting a count in an interval  $\delta t$ , and we have considered the fact that in  $N$  observation windows, there are  $\binom{N}{n} = \frac{N!}{n!(N-n)!}$  number of ways to record  $n$  counts. By letting  $N \rightarrow \infty$ ,  $\delta t \rightarrow 0$ , and Sterling's approximation  $N! \approx \sqrt{2\pi N} \left(\frac{N}{e}\right)^N$ , Equation 2 becomes

$$P(n, T) = \frac{(\lambda T)^n}{n!} \exp(-\lambda T) = \frac{n_{avg}^n}{n!} \exp(-n_{avg}) \quad (3)$$

which is the Poisson distribution for the probability of recording  $n$  counts in time  $T$ , where  $n_{avg} = \lambda T$  is the average number of photons counted in time  $T$ . Therefore, we

expect a constant-intensity light source to cause photoejections within the PMT, producing measurable photon counts, according to the statistical distribution of Equation 3.

A source of time dependent intensity will necessarily follow a more complex distribution. We are interested in the special case where light incident upon the detector is derived from a large number of independent and randomly phased sources, thus  $\lambda$  is no longer constant, and is instead a function of space and time. The result is a laser speckle pattern of granular appearance, which is due to the interference of light from the scattering centers. Photons arrive at the detector with greater probability when the net intensity is high, known as photon bunching, which causes the overall image to appear relatively brighter than when the net intensity is low. For such a speckle pattern, the probability that a randomly chosen image point will experience a photon count rate of  $\lambda$  is

$$P(\lambda) = \frac{1}{\lambda_{avg}} \exp\left(\frac{-\lambda}{\lambda_{avg}}\right) \quad (4)$$

where  $\lambda_{avg}$  is the average rate of incident photons over the entire image surface. Equation 3 is still a valid relationship for the probability of detecting  $n$  photons in time  $T$  when the incident rate is certainly  $\lambda$ , but now since  $\lambda$  is governed by its own probability distribution, the likelihood of detecting a count at  $\lambda$  is  $P(n, T)P(\lambda)$ . As  $\lambda$  can be zero or any positive real number, the total probability of recording  $n$  counts in time  $T$  is

$$P_{tot}(n, T) = \int_0^\infty P(n, T)P(\lambda)d\lambda = \int_0^\infty \frac{(\lambda T)^n}{n!} e^{-\lambda T} \frac{e^{-\lambda/\lambda_{avg}}}{\lambda_{avg}} d\lambda = \frac{n_{avg}^n}{(n_{avg} + 1)^{n+1}} \quad (5)$$

which is the Bose-Einstein distribution, where we have used the gamma function integral identity  $\int_0^\infty x^n e^{-ax} dx = n!/a^{n+1}$ . Therefore, we can determine whether a source is constant-intensity or psuedothermal in nature by comparing measured photon count statistics with Equation 3 and 5.

### 3 Procedures and Data

Our experimental apparatus, shown schematically in Figure 1, used a PMT of gain  $6.7 \times 10^6$  and a quantum efficiency 1.75% to detect photons emitted by a 633 nm HeNe laser, which releases on order of  $10^{18}$  photons per second according to its power output. This intensity would damage our detector, so we inserted an adjustable polarizer, to act as an attenuator, immediately following the laser output and used a microscope objective to expand the beam. Incoming photons are collimated by a metal tube before striking the photocathode and ejecting electrons, which are then accelerated into collisions with a series of alternating dynodes, all maintained at 1130 V, where each impact can eject multiple electrons, causing an electron cascade, which is then sent towards the next electrode. Ultimately a bunch of electrons, of number approximately equal to the PMT gain, land crash into the anode and create an amplified electrical signal. At this point, a current forms in the oscilloscope/counter circuit which passes across a resistor and creates a voltage pulse, then each pulse above the noise threshold represents a detection event.

As an ideal HeNe laser emits identical photons, it represents a constant intensity source when given a free path to the detector, so in order to create a psuedothermal

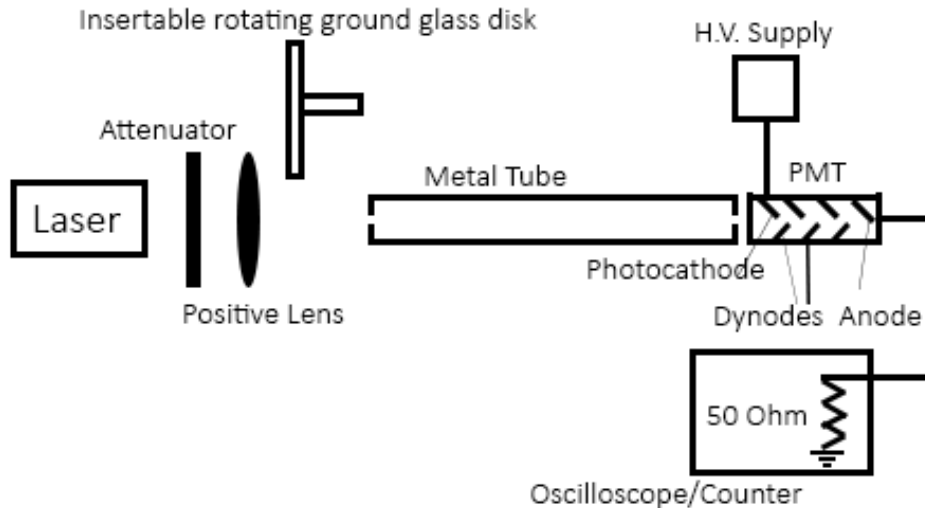


Figure 1: Block diagram of the experimental apparatus.

source, we inserted a ground glass disk in the path of the beam and used a small electric motor to rotate it along the optical axis with constant angular frequency such that the speckle pattern visibly drifts across the metal tube entrance. Ground glass creates uniform inhomogeneities, which then act as random scattering centers, while the disk rotation ensures that the emission phases vary randomly in time for all sources.

We first used an oscilloscope to observe the appearance of each event, shown in Figure 2, then switched to the photon counter for measurements. The  $-20$  mV pulses have a full width at half max of approximately  $t = 3$  ns, which is related to the PMT detection and multiplication process. Then, since the electrons pass across an  $R = 50 \Omega$  resistor to create a voltage pulse of approximately  $V = 20$  mV, we estimate the number of electrons of charge  $e$  in a PMT output pulse to be  $N = (I/e)t = (V/eR)t = 7.5 \times 10^6$ , which is in agreement with the manufacturer listed PMT gain of  $6.7 \times 10^6$  and the fact that a 633 nm photon has energy approximately 2 eV, which would only be enough to eject a single photoelectron. There is notable ringing of the pulses, especially for the largest peak, which we later filter from our measurements, along with background noise, through the introduction of a voltage discriminator. We suspect the ringing oscillation following a count is a result of the counter circuit recovering from the introduction of the nanosecond pulse of  $10^6$  electrons, but ringing may also be caused by electrons being thermally ejected from the anode, due to the voltage of its neighbor dynode, and any fluctuations in the anode potential that might result from sending such a quick pulse through the circuit, ultimately causing a back-current. Additionally, thermal ejections (towards the anode) can happen at any time, with frequency depending on the PMT temperature, and cause event like pulses, which are known as dark counts [1].

Across several oscilloscope traces, shown in Figure 3, there is significant fluctuation between the number of pulses in a given time window and the relative spacing of the pulses, which is representative of a statistical distribution for the number of counts within a short time interval, as expected. Additionally there is variation in pulse heights to some degree, although the typical pulses tend to be greater than 15 mV.

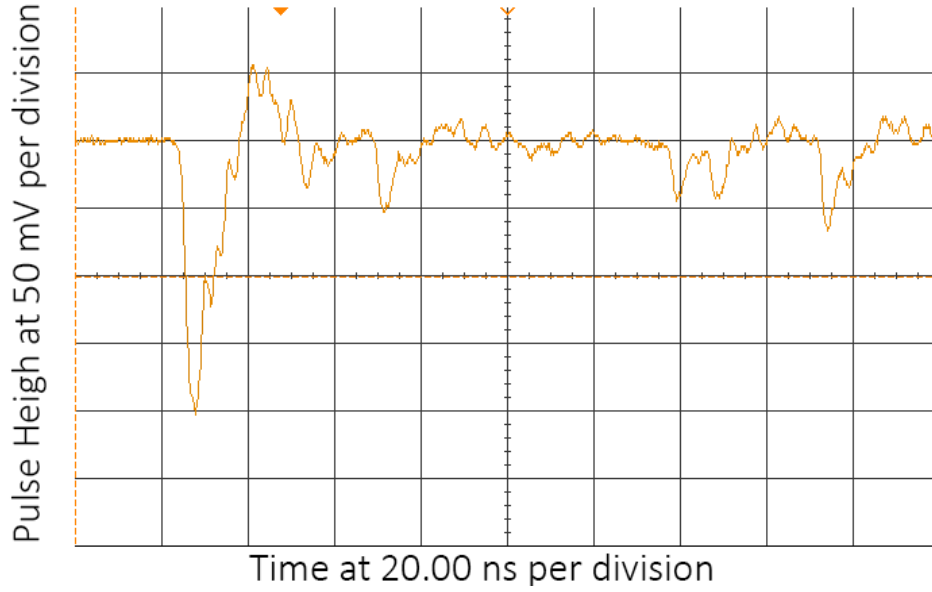


Figure 2: Oscilloscope display of a multiple sharp dip in voltage, which represent detection events. There is a single large dip of 200 mV and several more typical pulses of height approximately -20 mV.

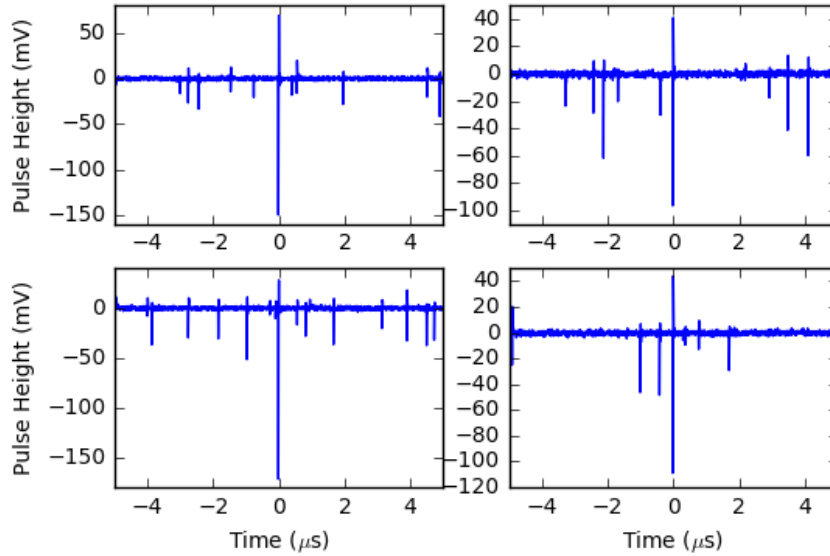


Figure 3: Comparison of multiple traces from the oscilloscope display at different times. Each dip into the negative voltage is a detection event, and any subsequent rise to positive voltage is ringing phenomena.

In order to determine the proper discriminator level, we measured the signal-to-noise ratio (real photon counts)/(noise counts) by recording the laser source count rate and background count rate as a function of the discriminator level. Then the difference between the laser counts and background counts provides the real counts, which is shown in Figure 4, along with with signal-to-noise ratio as a function of the discriminator voltage, where the discriminator voltage is negative because we desired to discard insufficiently deep pulses. As expected, the real counts increases linearly

with increasing discriminator voltage, since this corresponds to more lenient filtering, but there is a well defined peak of the signal-to-noise ratio near -10 mV, so we obtained the maximal signal-to-noise ratio of our apparatus by setting the discriminator voltage to -10 mV.

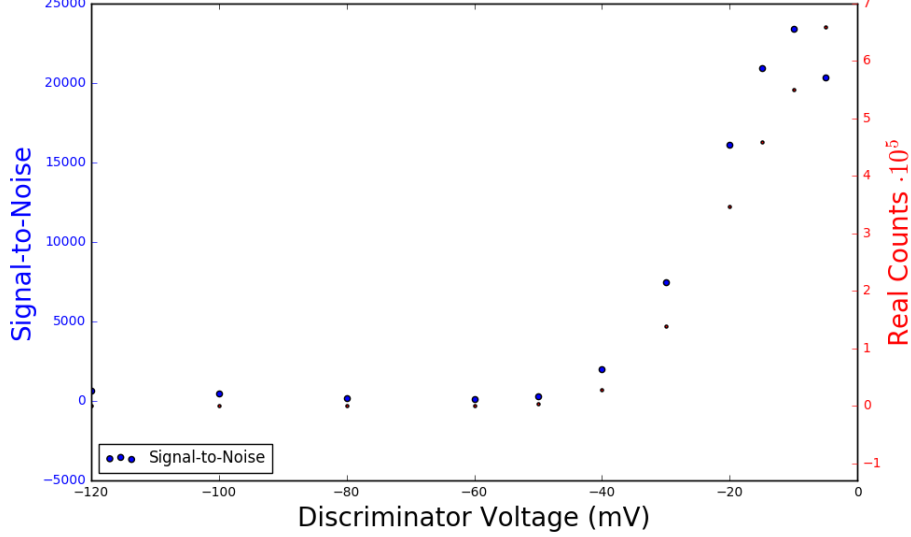


Figure 4: Scatter plot of the signal-to-noise ratio as a function of the discriminator voltage (on the left vertical axis) and the number of real photon counts as a function of the discriminator voltage (on the right vertical axis).

Once we found the optimal discriminator level, we used a Matlab program to communicate with the photon counter and set it to record the number of counts in 1000 1-msec windows, with zero delay between each interval, for the constant intensity scenario. We performed this process when the average count rate, as reported by the detector, was approximately 1,000, 3,000, and 10,000 counts per second, where we used the attenuator for rate adjustment, which are plotted as histograms in Figures 5, 6, and 7. Then, we inserted the rotating glass disk and performed the same process with at the same count rates, except now the dwell time between measurement windows was set to 300 ms, which ensured a unique speckle pattern for each measurement; histograms (in the form of a probability distribution) of this data is seen in Figures 8, 9, and 10.

## 4 Analysis and Discussion

By determining what fraction of our measurements had each count value, we constructed a probability distribution for the number of counts from both constant intensity and psuedothermal sources. Then, after determining the average number of counts recorded in each 1-msec window, we plotted the Poisson distribution of Equation 3 as an overlay on the constant intensity source distributions, and computed the chi square value for each data set. Note the Poisson distribution is in better agreement with the data for low count probabilities, which is as expected for counting experiments because the uncertainty value increases as the number of counts increases (although the fractional uncertainty decreases). For all three cases of constant intensity light,  $\chi^2$

is approximately  $1/2$ , placing these measurements in the 99% and above confidence region of agreement with the Poisson distribution, which is reflected by the fact that in Figures 5, 6, and 7, the Poisson distribution never lies further than two standard deviations from our measurements and more often than not, the Poisson distribution nearly passes through the center of the uncertainty bars. These results give certainty to our earlier claims that even for a constant intensity source of light incident upon the photocathode, photoelectrons are randomly ejected, and they serve as evidence for the laser source outputting constant amplitude, monochromatic, light.

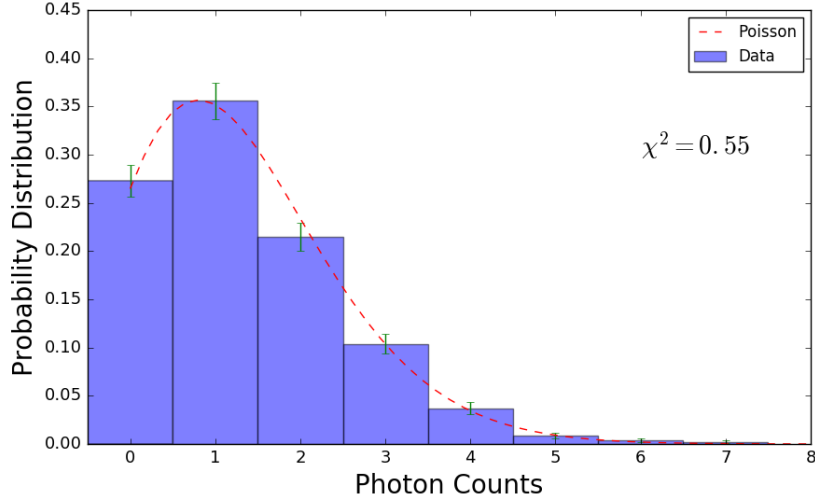


Figure 5: Histogram probability distribution for the number of counts within a 1-msec interval for a constant intensity source, with comparison to the predicted Poisson distribution for its average count rate of 1.33 counts per msec, and its associated chi square value.

We performed the same analysis for our rotating glass disk psuedothermal source, except now comparing with the Bose-Einstein distribution of Equation 5, which is shown in Figures 8, 9, and 10. In this case, the  $\chi^2$  values are significantly larger than in the constant intensity scenario, although they are still sufficiently near one that they are evidence for some agreement with the Bose-Einstein distribution, even though they differ from theory, on average, by two standard deviations. Upon inspection of Figures 8, 9, and 10, we notice that the Bose-Einstein distribution rises slower than the experimental data when approaching zero counts. None of these Figures have their largest peak in the zero count bin, which is contrary to the predictions of the Bose-Einstein distribution, and suggests that we do not have a perfectly thermal source. Causes for this could be inherent to the experiment, such as a portion of the laser beam traveling through the glass without being absorbed, which would introduce a low intensity Poisson distribution on top of the Bose-Einstein counts, or a poor choice of rotation speed for the glass disk.

## 5 Conclusion

We measured an agreement with 99% confidence between the Poisson distribution and our experimentally measured probability distribution for the number of photon

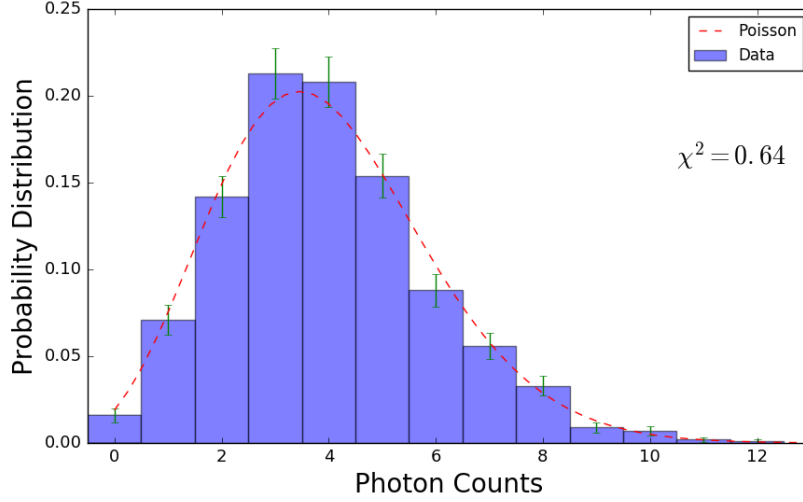


Figure 6: Histogram probability distribution for the number of counts within a 1-msec interval for a constant intensity source, with comparison to the predicted Poisson distribution for its average count rate of 3.97 counts per msec, and its associated chi square value.

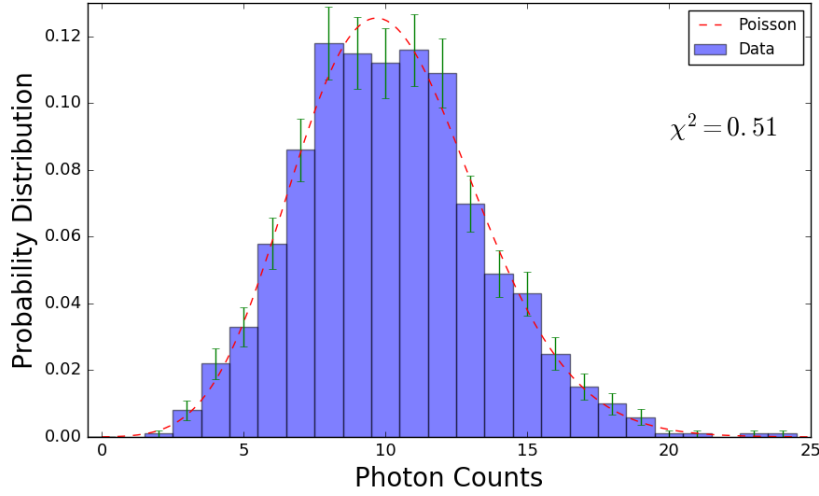


Figure 7: Histogram probability distribution for the number of counts within a 1-msec interval for a constant intensity source, with comparison to the predicted Poisson distribution for its average count rate of 10.2 counts per msec, and its associated chi square value.

counts recorded by the PMT when incident light was derived from a constant intensity laser source. We also found agreement between the Bose-Einstein distribution and the photon count probability distribution due to laser scattering off a glass disk, which provides psuedothermal light. From these observations, we conclude that our assumption that the probability of a photoejection event is linear with the rate of incoming photons, since we assumed this to derive the theoretical probability distributions, and that photon counts, which are the result of photoejections, are governed by

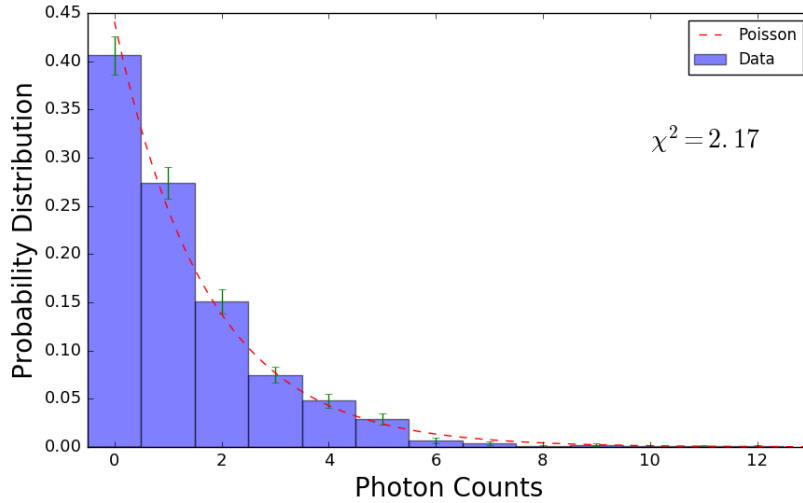


Figure 8: Histogram probability distribution for the number of counts within a 1-msec interval for a psuedothermal source, with comparison to the predicted Poisson distribution for its average count rate of 1.27 counts per msec, and its associated chi square value.

a stochastic process. While it appears as though some light passes through the glass disk unscathed, shifting our measured distribution slightly away from the pure Bose-Einstein situation, we have observed that, to good approximation, light scattered from a ground surface is thermal in nature, meaning the individual photons carry random phases and amplitudes, then their interference creates a speckle pattern.

Additionally our result for the number of electrons in each photopulse is approximately equivalent to the manufacturer listed gain of the PMT, which suggests that incoming photons from the laser are annihilated entirely when ejecting a single photon from the cathode. Also, we observed ringing of the PMT signal for about 10 ns after each pulse, which could cause the PMT to fail in detecting any photons during such a time window after a detection.

## References

- [1] P. Koczyk. Photon counting statistics. Undergraduate experiment. *American Journal of Physics*, 64(3):240, 1996.



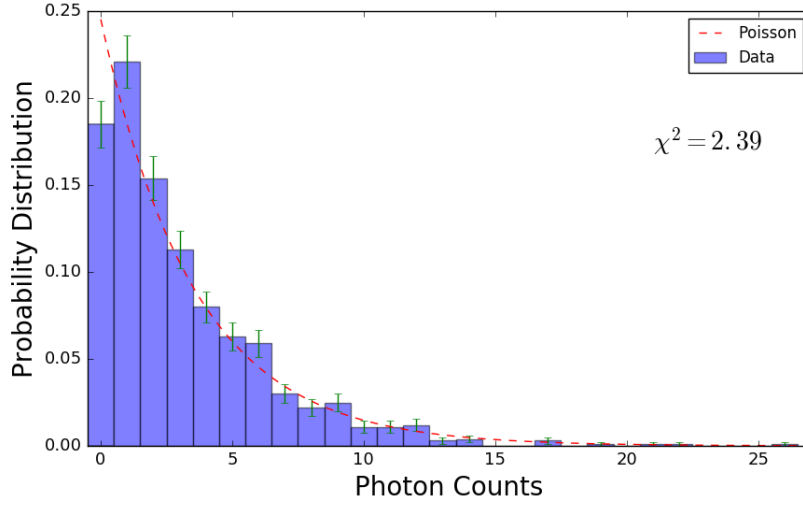


Figure 9: Histogram probability distribution for the number of counts within a 1-msec interval for a psuedothermal source, with comparison to the predicted Poisson distribution for its average count rate of 3.08 counts per msec, and its associated chi square value.

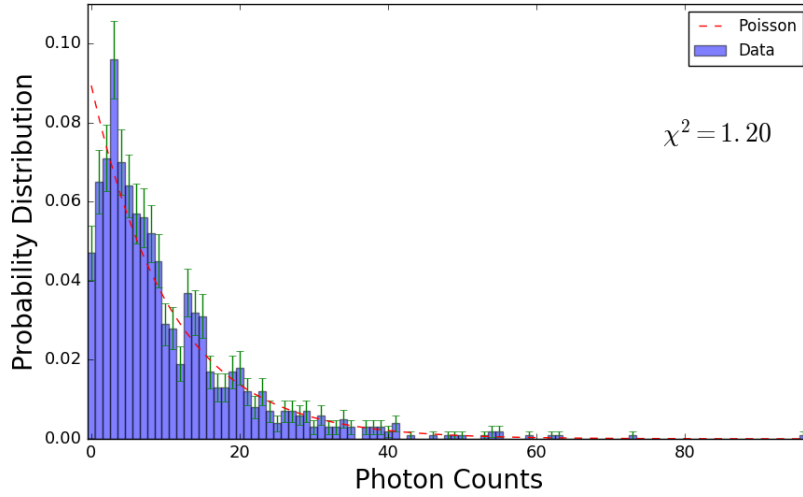


Figure 10: Histogram probability distribution for the number of counts within a 1-msec interval for a psuedothermal source, with comparison to the predicted Poisson distribution for its average count rate of 10.2 counts per msec, and its associated chi square value.